Am J Transl Res 2019;11(7):4100-4112
www.ajtr.org /ISSN:1943-8141/AJTR0089810

Original Article

Platelet-rich plasma in combination with adipose-derived stem cells promotes skin wound healing through activating Rho GTPase-mediated signaling pathway

Lei Zhang[1,2*], Baojian Zhang[3*], Boyu Liao[4], Sha Yuan[1], Yanqun Liu[3], Zhengyin Liao[4], Biao Cheng[1]

[1]Department of Plastic Surgery, General Hospital of Southern Theater Command, PLA, Guangzhou 510010, China; [2]Institute of Huabo Biopharmaceutical, Guangzhou 510010, China; [3]Department of Orthopedics, Yanbian University Hospital, Yanji 133000, China; [4]Department of Interventional Oncology, West China Hospital, Chengdu 610041, China. [*]Equal contributors.

Received December 13, 2018; Accepted May 6, 2019; Epub July 15, 2019; Published July 30, 2019

Abstract: Adipose-derived stem cells (ADSCs) are multipotent stromal cells that provide an abundant source of cells for skin tissue engineering and wound healing. Platelet-rich plasma (PRP) is a concentrate of platelet-rich plasma protein, which contains several different growth factors and other cytokines. In this study, we combined ADSCs with PRP for wound healing. Herein, we found ADSCs in combination with PRP was able to promote wound healing, granulation formation, collagen deposition and re-epithelialization. The mechanism exploration discovered that PRP promoted stress fiber formation in ADSCs, leading to cell migration. Then, we demonstrated that PRP enhanced the expression of Rho GTP family proteins, including Cdc 42, Rac 1 and Rho A. Moreover, it promoted the expression of downstream Rho GTP signaling molecules, including PAK 1, ROCK 2, LIMK 1 and Cofilin. When PRP was used in combination with the Cdc 42 inhibitor ZCL278, the Rho A inhibitor CT04, Rac 1 inhibitor NSC23766, PAK inhibitor FRAX597, or Rock 2 inhibitor Y27632 to treat ADSCs, stress fiber formation was significantly reduced, resulting in decreased cell migration. Our findings may provide a promising approach to promote wound healing.

Keywords: ADSCs, platelet-rich plasma, migration, Rho GTPases, wound healing

Introduction

In undamaged skin, the epidermis and dermis form a protective barrier against the external environment. When the barrier is broken, an orchestrated cascade of biochemical events is set into motion to repair the damaged skin [1]. However, large skin wounds and chronic wounds cannot self-heal adequately because of limited cell sources [2]. Mesenchymal stem cells (MSCs) are multipotent stromal cells that can differentiate into a variety of cell types, including osteoblasts (bone cells), chondrocytes (cartilage cells), myocytes, adipocytes and skin cells [3]; therefore, they can be an optimal alternative cell source that may be used for skin wound healing. Among the many types of MSCs, adipose-derived stem cells (ADSCs) are the most commonly used in dermatology [4]. Fat tissue is an excellent source of MSCs [5]. The isolation of ADSCs is very simple and highly efficient: the cellular yield is 100-1000 times greater than that of bone mesenchymal stem cells (BMSCs) [6]. It has been shown that ADSCs can directly or indirectly (by its paracrine effect, releasing cytokines and growth factors) participate in and promote the regeneration process [7]. In addition, ADSCs can be used in combination with growth factors to enhance wound healing by inducing angiogenesis and stimulating collagen deposition [8, 9].

Platelet-rich plasma (PRP) is a concentrate of platelet-rich plasma protein derived from whole blood, centrifuged to remove red blood cells [10]. As a concentrated source of blood plasma and autologous conditioned plasma, PRP con-

tains several different growth factors and other cytokines, including platelet-derived growth factor (PDGF), transforming growth factor beta (TGF-β), fibroblast growth factor (FGF), insulin-like growth factor 1 (IGF-1), insulin-like growth factor 2 (IGF-2), vascular endothelial growth factor (VEGF), epidermal growth factor (EGF), Interleukin 8 (IL-8), keratinocyte growth factor (KGF), connective tissue growth factor (CTGF) [11-13]. It has been used to encourage a brisk healing response across several specialties, in particular plastic surgery, dentistry, orthopedics and dermatology [14]. For stem cell transplantation, PRP is capable of providing enough nutritions for transplanted stem cells.

In our previous study, we used ADSCs in combination with growth factors to co-treat skin wounds, and this combination therapy significantly accelerated wound healing. Further mechanism studies have revealed that growth factors can activate the JNK and ERK signaling pathway to induce actin stress fiber formation, thereby promoting ADSC migration to enhance wound healing [15]. Accumulating evidence demonstrates that Rho GTPases play an important role in cell migration [16]. Thus, in this study, we used PRP to replace growth factors, we tested wound healing effects of PRP in combination with ADSCs, and we also tested whether PRP was able to promote ADSCs migration. In addition, we explored whether PRP induced ADSC migration via Rho GTPases. We detected the expression of Rho family proteins, including Cdc 42, Rac 1 and Rho A, and the expression of downstream molecules in ADSCs treated with PRP. The present study may reveal more about the mechanism of PRP induced ADSC migration.

Materials and methods

Isolation and identification of ADSCs

Inguinal adipose tissues were isolated from 12-14-week-old female BALB/c mice and digested at 37°C in phosphate-buffered saline (PBS) containing 2% bovine serum albumin (BSA) and 2 mg/ml collagenase (collagenase A, Roche), for 15-20 min. After filtration through a 40 μm nylon filter mesh (BD Falcon) and centrifugation, the isolated cells were suspended in medium, counted with a hemocytometer, plated at 5×10^4 cells/ml in 6 cm tissue culture plates, and cultured at the presence of 20% fetal bovine serum (FBS)-containing Dulbecco's modified Eagle's medium (DMEM). The cells were observed daily under an inverted phase-contrast microscope and were passaged at 80-90% confluence. The culture media was changed every two days.

Blood collection and platelet-rich plasma preparation

The platelet-rich plasma was obtained by centrifugation of 50 ml fresh blood at 250 × *g* at 37°C for 15 minutes, about 20 ml platelet-rich plasma was obtained after centrifugation.

Wound healing

Forty-eight healthy adult specific-pathogen-free (SPF)-class C57BL/6 mice were randomized into 4 groups: control group, PRP group, ADSC group and PRP + ADSCs group. The mice were anesthetized by intraperitoneal injection of 10% chloral hydrate (0.003 ml/g). After the hair on two sides of the back of each C57BL/6 mouse was shaved, the remaining hair was removed using frozen honey wax. Next, a square-shaped (1 cm^2) full-thickness wound was created. Totally 0.4 ml PBS (control), 0.4 ml PRP, 0.4 ml ADSCs (1×10^6/ml), 0.4 ml PRP + ADSCs (1×10^6/ml) were used for each wound of each group. After the operation, the mice had free access to food and water. The healing of the wounds on each mouse was recorded using a digital camera on the day of the operation and again on days 3, 5, 7 and 14 after the operation. The wound-healing rates were calculated using the following equation: wound-healing rate = (the area of the original wound - the area of the unhealed wound)/the area of the original wound × 100%. The Bioethics Committee of Southern Medical University approved all animal experiments, and experiments were performed in accordance with the National Institutes of Health (NIH) Guide for the Care and Use of Laboratory Animals.

Transwell assay

ADSCs at passage 4 were serum starved for 12 h, resuspended in serum-free medium, and adjusted to a density of 1×10^6 cells/ml. One hundred microliters of ADSCs was placed in the upper chamber of a Transwell plate (Corning, Corning, NY, USA). Serum-free L-DMEM, with or without PRP, was added to the lower chamber. Prior to the addition of the ADSCs, preheated serum-free L-DMEM (300 μl) was added to the

upper chamber and allowed to incubate for 1 h at 37°C. After the ADSCs were incubated for 24 h at 37°C, the cells that had migrated to the lower chambers were collected, stained with crystal violet (Beyotime, Haimen, China), and photographed (20 ×); five samples from each group were selected for counting.

Wound scratch assay

ADSCs at passage 4 were seeded in 12-well plates at a density of 4-5 × 10^5 cells per well. When the cells grew to 90% confluence, the medium was aspirated away, and the cells were serum starved for 12 h. The cells were divided into control (PBS) and PRP treated groups. A scratch wound was created with a micropipette tip. The wounds were photographed 0, 12, 24, 36, 48, 60, and 72 h after wounding. The assays were performed in quadruplicate.

Immunofluorescence staining

ADSCs at passage 4 were seeded at a density of 4 × 10^5 cells/well in 24-well plates (Corning) with a coverslip (Fisher Scientific, Shanghai, China). The cells were serum starved for 12 h and divided into eight treatment groups. The negative and positive control treatments consisted of incubation in DMEM containing PBS or PRP, respectively. After 30, 120, 240, or 360 min of treatment, the coverslips were removed, and the cells were fixed in 4% PFA, permeabilized with 0.1% Triton X-100 for 5 min, blocked with 1% BSA for 20 min at room temperature, and stained with phallotoxins (phalloidin; Invitrogen). After washing with PBS, the cells were counterstained with Hoechst 33258 (dilution 1:500) for 10 min, washed again with PBS, mounted, and examined by fluorescence microscopy.

Pull-down assay and western blot

The GTPase pull-down assay was performed according to the manufacturer's protocol (Rho Assay Reagent (Rhotekin RBD, Agarose), Millipore, cat. #14-383). ADSCs at passage 4 were cultured in a 100 mm Petri dish to approximately 85-90% confluence. The cells were serum starved overnight and then stimulated with PRP for 15, 30 or 120 min. The cells were then washed with ice-cold Tris-buffered saline (TBS) and lysed with ice-cold Mg^{2+}-containing buffer (MLB: 25 mM HEPES, pH 7.5, 150 mM NaCl, 1% Igepal CA-630, 10% glycerol, 25 mM NaF, 10 mM $MgCl_2$, 1 mM EDTA, 1 mM sodium orthovanadate and 1 mM PMSF). The cells were rapidly scraped off the plates, and the lysates were transferred to prechilled Eppendorf tubes. Protein concentrations were determined via a bicinchoninic acid assay (Beyotime, P0009). The cell lysates were assayed for total Rho A (1:200; Santa Cruz; SC418), p-Limk1 (1:500; Sigma; SAB4300103), Limk1 (1:1000; Cell Signaling; #3842), p-Limk2 (1:500; Sigma; SAB4300104), Limk2 (1:1000; Cell Signaling; #3844), p-Cofilin (1:1000; Cell Signaling; #3311), and Cofilin (1:1000; Cell Signaling; #3312). Another aliquot of cell lysates was subjected to a Rhotekin binding assay as follows: the cell lysates were centrifuged at 14,000 × g for 5 min at 4°C. Equal amounts of cleared cell lysates were incubated with GST-Rhotekin agarose at a final concentration of 30 μg/ml at 4°C for 45 min with gentle agitation, followed by brief centrifugation at 14,000 × g for 10 s at 4°C. The supernatants were removed and discarded. The bead pellets were washed three times by centrifuging at 5000 rpm for 20 s with 0.5 ml of ice-cold MLB. The beads were resuspended in 40 μl of 2 × Laemmli sample buffer and boiled for 5 min. The beads were pelleted by brief centrifugation, and the supernatants were analyzed by western blot using anti-Rho A antibodies and secondary antibodies (goat anti-rabbit IgG, 1:1000, Millipore, Cat. #AP-132P; goat anti-mouse IgG, 1:1000, Millipore, Cat. #AP124P). The bands were visualized using enhanced chemiluminescence (ECL) detection system and quantified using Quantity One software (Bio-Rad, Hercules, CA, USA).

Histological observations

After 3, 5, 7, 10 days treatment, the skin in the central area of suckling mouse back was carefully excised, rinsed in PBS, and then fixed in 4% Paraformaldehyde (PFA). Samples were dehydrated in a graded ethanol series (70-100%) and embedded in paraffin. Five-micrometer sections were prepared. According to the standard procedures, samples were stained with either hematoxylin and eosin (HE) or Masson trichrome.

Statistical analyses

Statistical analysis was performed using Statistical Package for the Social Sciences (SPSS) software version 13.0. All the data are expressed in the form of mean value ± standard

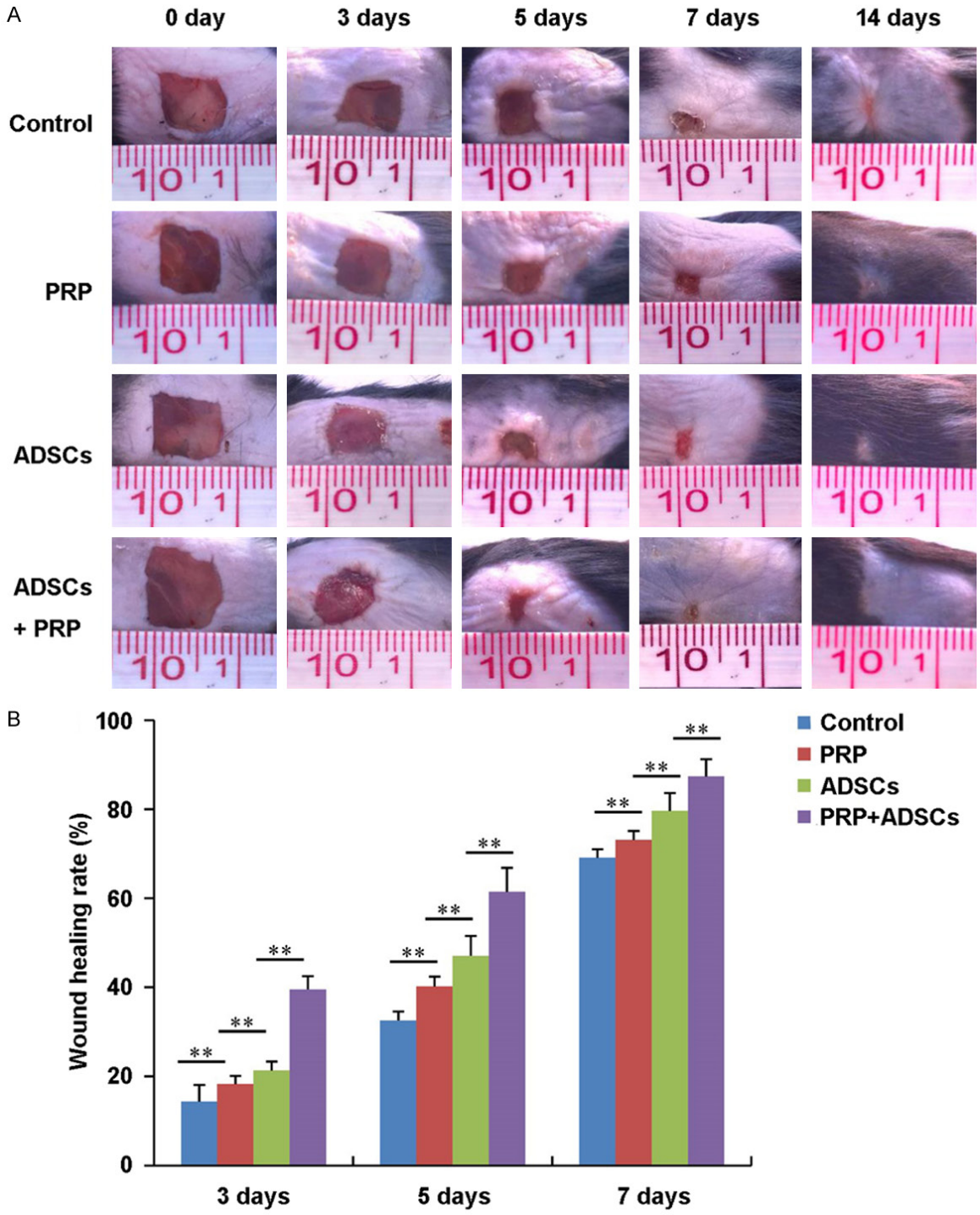

Figure 1. General observations of wound healing of control, PRP, ADSCs and ADSCs + PRP treated group. A. Photograph of wound of control, PRP, ADSCs and ADSCs + PRP treated group after 0, 3, 5, 7, 14 days treatment respectively. B. The wound healing rate of control, PRP, ADSCs and ADSCs + PRP treated group after 0, 3, 5, 7, 14 days treatment (n = 3). **P < 0.01.

deviation. Differences among three or four groups were assessed using one-way ANOVA followed by Fisher's Least Significance Difference test. A value of $P < 0.05$ was considered statistically significant (significance levels: *P < 0.05 and **P < 0.01).

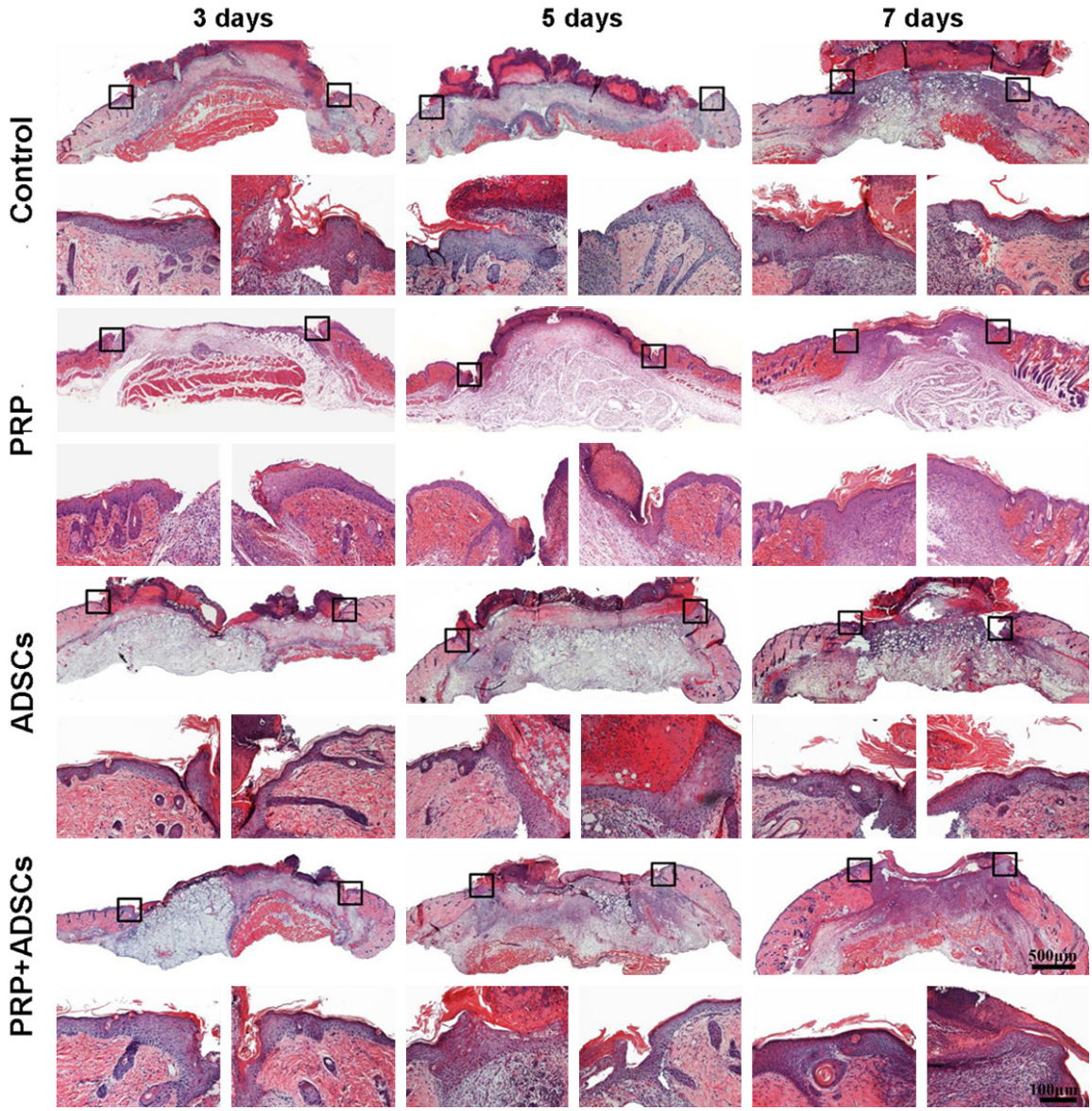

Figure 2. The histological observations of wound of control, PRP, ADSCs and ADSCs + PRP treated group after 3, 5, 7 days treatment respectively. The magnification pictures were left and right edge of each wound respectively.

Results

PRP in combination with ADSCs treatment promotes wound closure

Figure 1A shows the general observations of wound healing of control, PRP, ADSCs, PRP in combination with ADSCs treated group respectively. After 3 days of treatment, there was no significant difference in wound closure among control, PRP and ADSCs treated groups. While the wound closure rate was obviously higher in PRP in combination with ADSCs treated group compared to the other 3 groups ($P < 0.01$) (**Figure 1B**). After 5 days of treatment, the wound closure rate in PRP and ADSCs treated groups was higher than the control group ($P < 0.01$). And PRP in combination with ADSCs treated group had the highest wound closure rate. After 7 days of treatment, the wounds in PRP in combination with ADSCs treated group had completed closure. While the wounds in other 3 groups still did not closure.

PRP in combination with ADSCs treatment promotes granulation tissue formation and re-epithelialization

Figure 2 shows the granulation tissue formation and re-epithelialization of control, PRP,

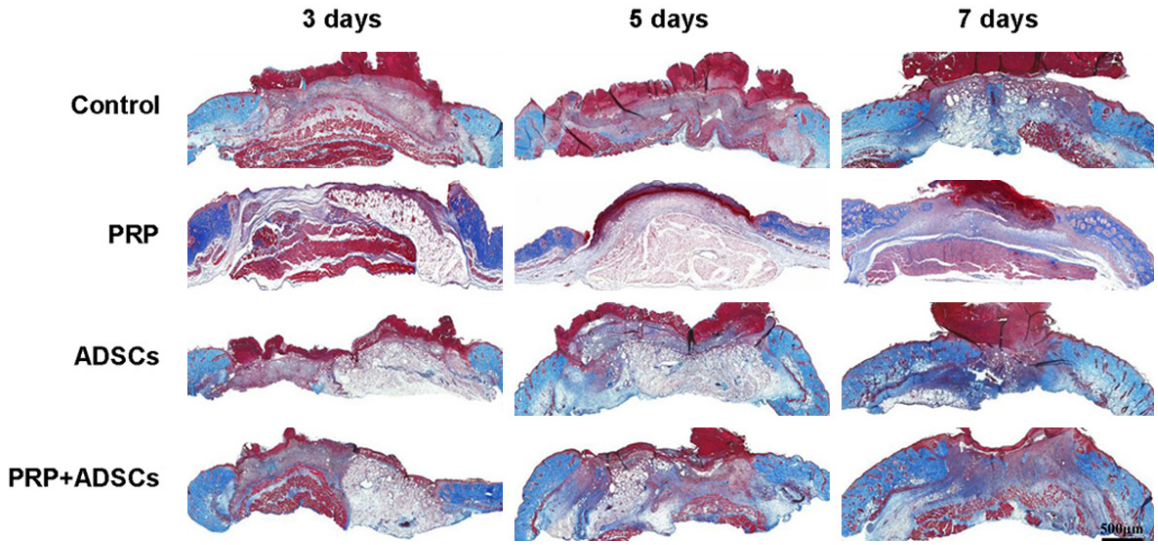

Figure 3. The Masson trichrome staining of wound of control, PRP, ADSCs and ADSCs + PRP treated group after 3, 5, 7 days treatment respectively.

ADSCs, PRP in combination with ADSCs treated group respectively. After 3 days of treatment, granulation tissue started to form in PRP in combination with ADSCs treated group. While, visible granulation tissue formation could be seen in control, PRP, ADSCs groups after 7 days of treatment. In addition, the wounds of PRP in combination with ADSCs treated group was full filled with granulation tissue, while the wounds of other 3 groups still had some areas without granulation tissue formation. Moreover, the re-epithelialization of wounds of PRP, ADSCs, PRP in combination with ADSCs treated groups were better than the control group at each indicated time point. By comparison, among the PRP, ADSCs, PRP in combination with ADSCs treated groups, the PRP in combination with ADSCs treated group had best re-epithelialization at each indicated time point.

PRP in combination with ADSCs treatment promotes collagen deposition

Following, we examined the collagen deposition at the wound site of control, PRP, ADSCs, PRP in combination with ADSCs treated group respectively. As shown in **Figure 3**, after 3 days of treatment, more collagen fibers could be detected in PRP in combination with ADSCs treated group compared to the other 3 groups. After 5 days of treatment, more collagen fibers could be seen in both ADSCs and PRP in combination with ADSCs treated groups compared to control and PRP groups. After 7 days of treatment, the wounds of PRP in combination with ADSCs treated group full filled with new deposited collagen fibers, while wounds of other 3 groups still had some area without collagen deposition.

PRP promotes ADSCs migration by inducing actin stress fiber formation

Firstly, we found that PRP could promote ADSC invasion after 24 hours of induction *in vitro* (**Figure 4A**). In addition, the scratch wound healing results showed that after 36 hours of treatment, the wound healing rate of ADSCs treated with PRP was significantly higher than that of the control group, and after 72 hours, the gap was fully filled by ADSCs, while the wound in the control group had not closed (**Figure 4B**). Actin stress fibers have a crucial role in cell migration and contraction, so we used phallotoxin (phalloidin) staining to examine the distribution and formation of actin stress fibers in ADSCs treated with PRP. As shown in **Figure 4C**, more actin stress fibers were observed with 30 minutes of treatment with PRP than with PBS treatment, and they were distributed along the membrane. After 2 and 4 h of treatment, numerous actin stress fibers were arranged across the cell bodies. After 6 h of treatment, only a few actin stress fibers were seen at the periphery of the cells.

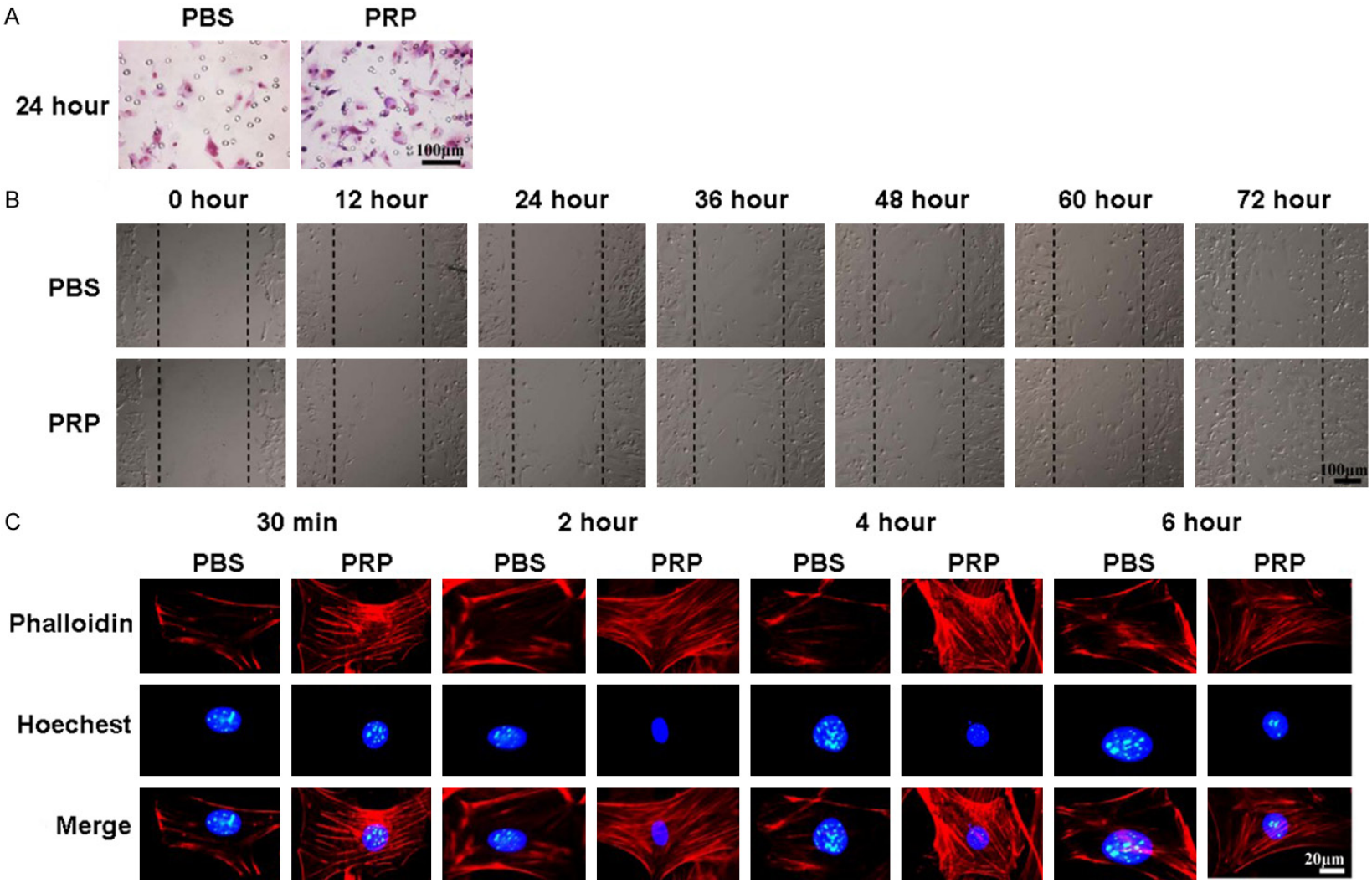

Figure 4. PRP induces actin stress fiber formation and ADSC migration. A. Transwell assay showing ADSCs that invaded after treatment with PBS or PRP. B. The scratch wound healing assay of ADSCs treated with PRP for different lengths of time. C. Phallotoxin staining (phalloidin) was performed to stain actin in ADSCs treated with PBS or PRP; nuclei were counterstained with Hoechst 33258.

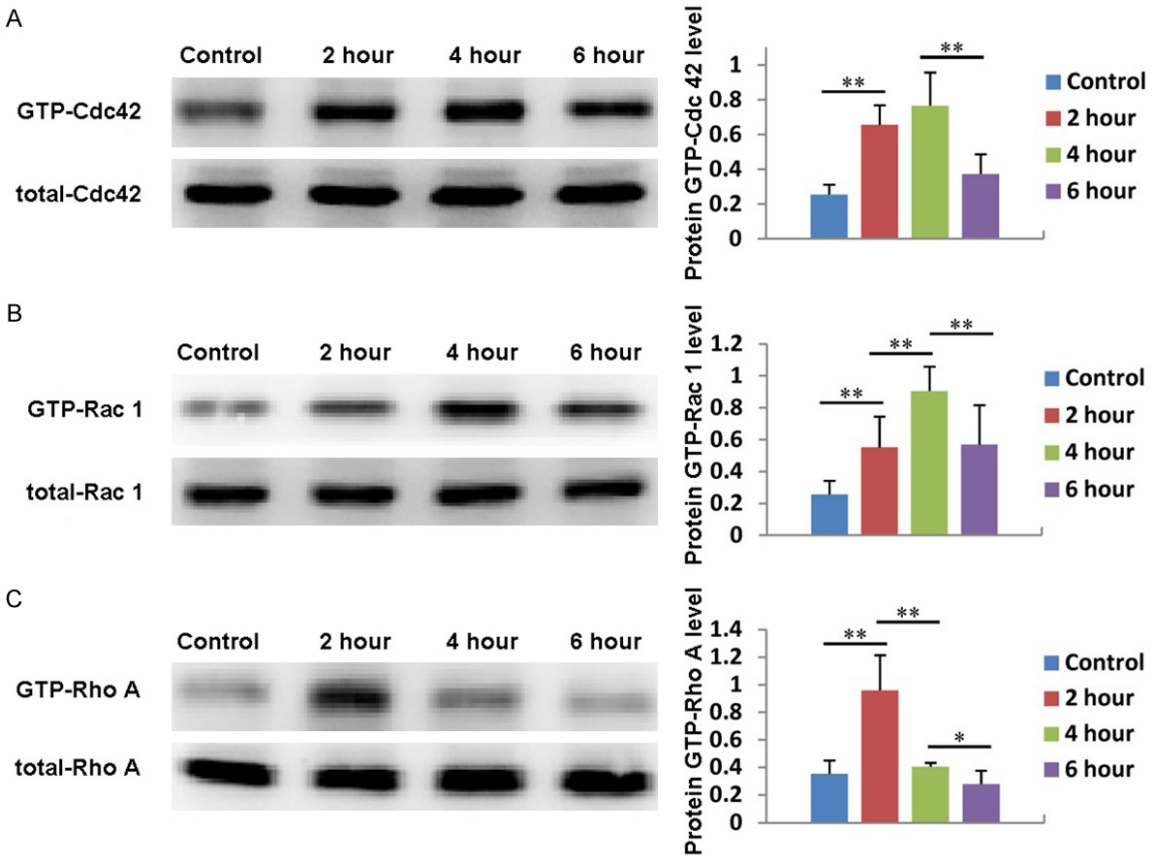

Figure 5. Rho family proteins are involved in PRP induced ADSC migration. The expression and quantification of Cdc 42 (A), Rac 1 (B) and Rho A (C) in ADSCs treated with PRP for 2, 4, or 6 hours. Untreated cells served as controls.

Rho family proteins are involved in PRP induced ADSC migration

Rho family proteins, such as Cdc 42, Rac 1 and Rho A, play an important role in cytoskeletal reorganization and decomposition, which directly affect cell migration. Therefore, in this study, we first investigated whether PRP induced ADSC migration through Rho family proteins. As shown in **Figure 5A**, the expression of Cdc 42 in ADSCs treated with PRP gradually increased compared with that in the untreated group. It reached its maximum level after 4 hours of treatment and then fell back to its normal level. Similarly, the expression of Rac 1 also gradually increased, reached its maximum value at 4 hours, then decreased (**Figure 5B**). The expression of Rho A achieved its highest level after 2 hours of treatment and then decreased to its normal level (**Figure 5C**). These results suggest that the Rho family proteins Cdc 42, Rac 1, and Rho A are involved in PRP induced ADSC migration.

The expression of Rho GTPase downstream signal molecules

We have already demonstrated that PRP can regulate the expression of Cdc 42, Rac 1 and Rho A; therefore, we also explored whether the expression of downstream signaling molecules, including PAK 1, ROCK 2, LIMK 1 and Cofilin, is affected by PRP. As shown in **Figure 6A**, the expression of PAK 1 gradually increased in ADSCs treated with PRP, reached its highest level at 4 hours, then decreased at 6 hours. In addition, the expression of PAK 1 could be significantly inhibited by the Cdc 42 inhibitor ZCL278 and the PAK inhibitor FRAX597 (**Figure 7A**). ROCK 2 expression also increased with PRP treatment, reaching its maximum value at 4 hours and then decreasing (**Figure 6B**). Additionally, the expression of ROCK 2 could be significantly suppressed by the Rho A inhibitor CT04 and the Rock 2 inhibitor Y27632 (**Figure 7B**). Moreover, the expression of LIMK 1 gradually increased from 0 to 6 hours after PRP addi-

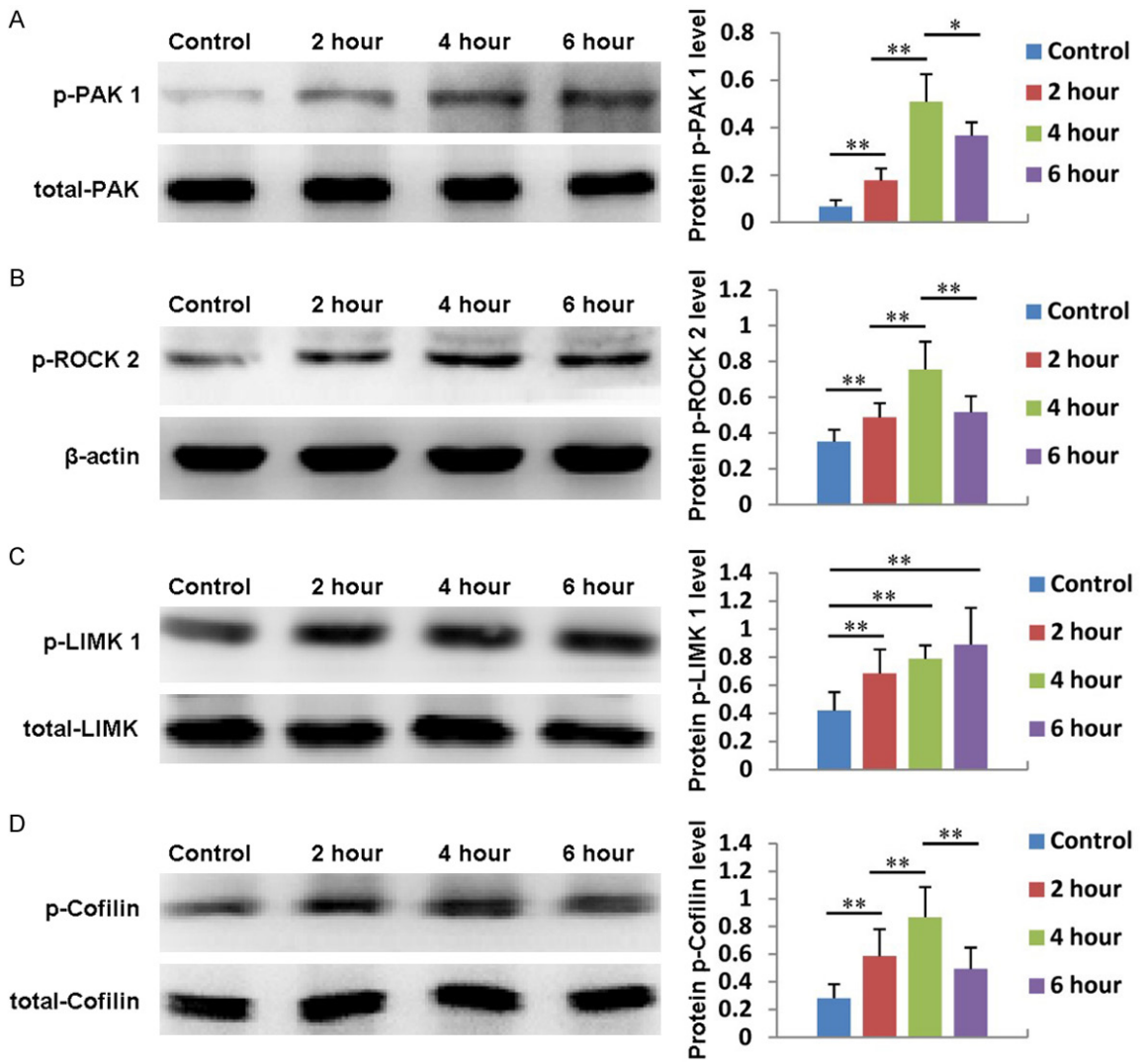

Figure 6. The expression and quantification of of PAK 1 (A), ROCK2 (B), LIMK 1 (C) and Cofilin (D) in ADSCs treated with PRP for 2, 4, or 6 hours. Untreated cells served as controls.

tion (**Figure 6C**). The expression of Cofilin also increased after PRP addition, reached its highest level at 4 hours, then decreased at 6 hours (**Figure 6D**). Furthermore, the expression levels of LIMK 1 and Cofilin were inhibited by the Cdc 42 inhibitor ZCL278, the PAK inhibitor FRAX597, the Rho A inhibitor CT04, the Rock 2 inhibitor Y27632 and the Rac 1 inhibitor NSC23766 (**Figure 7C** and **7D**). These results indicate that PRP also affects the expression of PAK 1, ROCK 2, LIMK 1 and Cofilin.

The effects of Rho GTPase downstream signaling molecules on ADSC actin stress fiber formation and migration

After we demonstrated that PRP could activate Rho GTPase family proteins, including Cdc 42, Rho A and Rac 1, and their downstream signaling molecules PAK 1, Rock 2, LIMK 1, and Cofilin, we further explored whether PRP induced ADSC migration via Rho GTPase family members and their downstream signaling molecules. As shown in **Figure 8A**, the Transwell invasion results clearly showed more ADSC migration after treatment with PRP than in the control group ($P < 0.01$). However, when ADSCs were co-treated with PRP and the Cdc 42 inhibitor ZCL278, the PAK inhibitor FRAX597, the Rho A inhibitor CT04, the Rock 2 inhibitor Y27632, or the Rac 1 inhibitor NSC23766, the migration was significantly lower than that in the group treated with PRP alone ($P < 0.01$) and were not significantly different from that of the control group. Then, we tested whether these inhibi-

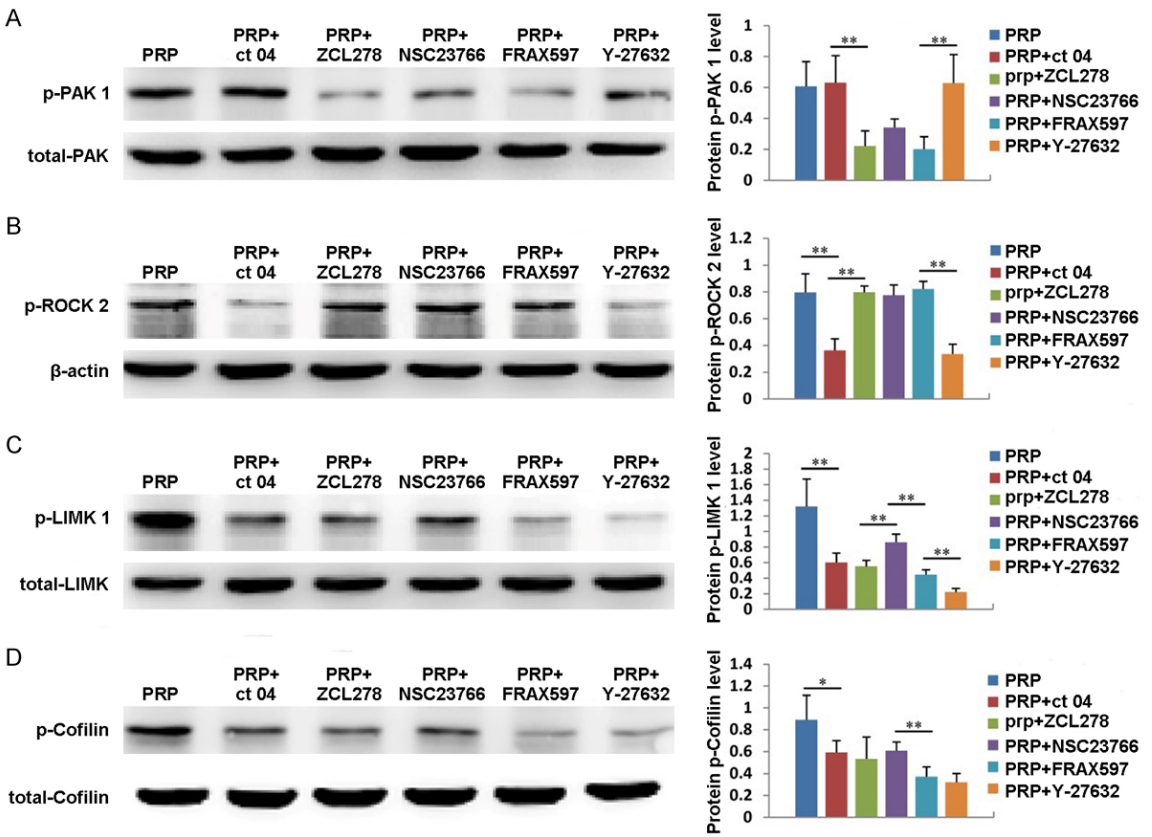

Figure 7. The expression and quantification of PAK 1 (A), ROCK2 (B), LIMK 1 (C) and Cofilin (D) in ADSCs treated with PRP plus the Cdc 42 inhibitor ZCL278, the PAK inhibitor FRAX597, the Rho A inhibitor CT04, the Rock 2 inhibitor Y27632 or Rac 1 inhibitor NSC23766. Untreated cells served as controls.

tors were capable of suppressing actin stress fiber formation in ADSCs after treatment with PRP for 2 hours. As shown in **Figure 8B**, more actin stress fibers were observed along the membrane after treatment with PRP for 2 hours than after PBS treatment. However, there were no significant differences in actin stress fiber formation before and after the ADSCs were co-treated with PRP in combination with the Cdc 42 inhibitor ZCL278, the Rho A inhibitor CT04, or the Rac 1 inhibitor NSC23766. Moreover, an obvious inhibitory effect was observed in ADSCs co-treated with PRP in combination with the PAK inhibitor FRAX597 or the Rock 2 inhibitor Y27632. In the wound scratch assay, when compared with the control group, in the PRP treated group, many migrated ADSCs were observed. By contrast, only a few migrated ADSCs could be seen in the scratch in the groups co-treated with PRP and the Cdc 42 inhibitor ZCL278, the PAK inhibitor FRAX597, the Rho A inhibitor CT04, the Rock 2 inhibitor Y27632, or the Rac 1 inhibitor NSC23766. This was especially true in the PRP + FRAX597 group and the PRP + Y27632 group (**Figure 8C**).

Discussion

Cell migration is an essential process in all multicellular organisms and is important not only during development but also throughout life, such as during wound healing. In animals, cell migration is guided by extracellular cues acting as either attractants or repellants. These cues may be soluble factors that can act at a distance or they may be local signals received from neighboring cells or the extracellular matrix. They elicit a large variety of intracellular responses, including changes in the organization of the actin and microtubule cytoskeletons, in vesicular transport pathways and in gene transcription [16]. PRP contains several different growth factors and other cytokines, including PDGF, TGF-β, FGF, IGF-1, IGF-2, VEGF, EGF, IL-8, KGF. The contained TGF-β [17], FGF [18], EGF [19] are able to promote cell migration. In

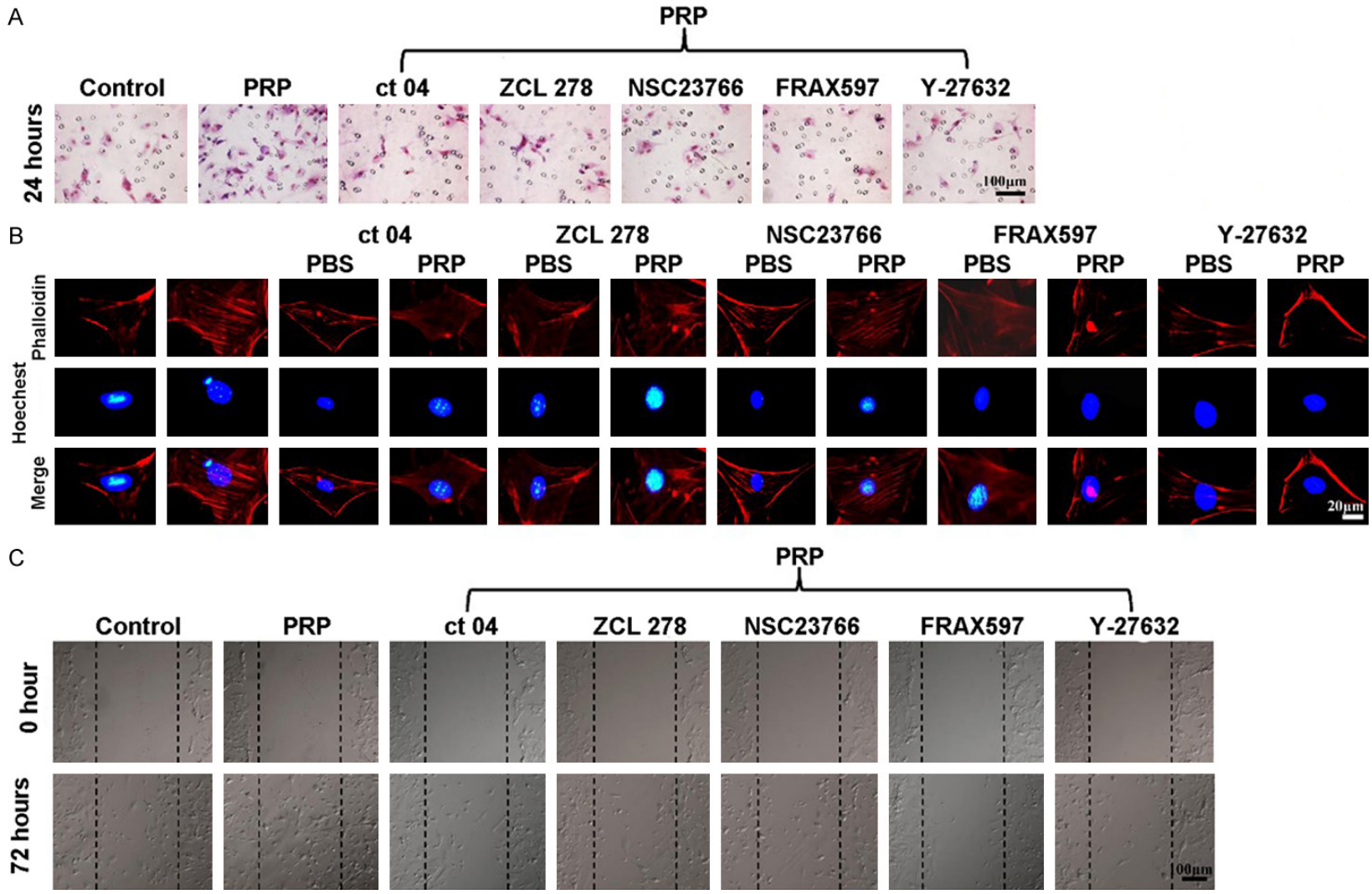

Figure 8. The effects of downstream Rho GTPase signaling molecules on ADSCs, actin stress fiber formation and migration. A. Transwell assay and quantification of ADSCs treated with PBS, PRP, PRP + ZCL278, PRP + NSC23766, PRP + CT04, PRP + Y27632 or PRP + FRAX597 (n = 6). B. Phallotoxin staining (phalloidin) was performed to stain actin in ADSCs treated with PBS, PRP, PRP + ZCL278, PRP + NSC23766, PRP + CT04, PRP + Y27632 or PRP + FRAX597; nuclei were counter-stained with Hoechst 33258 (n = 6). C. Scratch wound assay and quantification of ADSCs treated with PBS, PRP, PRP + ZCL278, PRP + NSC23766, PRP + CT04, PRP + Y27632 or PRP + FRAX597 (n = 6). *P < 0.05, **P < 0.01.

the current study, we discovered that PRP was able to promote ADSC migration through the Rho GTP-LIMK1-Cofilin signaling pathway.

LIM kinase 1 (LIMK1) belongs to a novel dual specificity (serine/threonine and tyrosine) kinase family and contains two amino-terminal LIM domains [20]. Cofilin, an actin-binding protein that is considered a potent regulator of actin dynamics due to its activity in F-actin depolymerization, is the only known substrate of LIMK1. The function of Cofilin is inhibited by phosphorylation at the Ser-3 residue by LIMK1, which leads to the accumulation of F-actin (Pollard and Borisy, 2003).

The catalytic activity of LIMK1 is regulated by distinct members of the Rho subfamily of small GTPases (Rho, Rac, and Cdc42), which controls actin filament dynamics and focal adhesion assembly in response to extra- and intracellular stimuli. Rho, Rac, and Cdc42 induce the formation of stress fibers, the assembly of lamellipodia and membrane ruffles, and the regulation of filopodial protrusions, respectively [21]. LIMK1 has been shown to specifically mediate Rac-induced actin cytoskeletal reorganization and focal adhesion complexes [22, 23]. The Rac-induced activation of LIMK1 is mediated by PAK1, which phosphorylates LIMK1 on its Thr508 residue [24]. Other studies have also proposed that Rho- and Cdc42-induced cytoskeletal changes are mediated through the phosphorylation of LIMK1 by the Rho-dependent protein kinase ROCK and the Cdc42-regulated protein kinase PAK4 [25, 26].

Our results are consistent with these previously reported results. We first demonstrate that PRP can enhance the expression of Rho GTP family proteins, including Cdc 42, Rac 1 and Rho A. Moreover, it can also promote the expression of Rho GTP downstream signaling molecules, including PAK 1, ROCK 2, LIMK 1 and Cofilin. When PRP is used in combination with the Cdc 42 inhibitor ZCL278, the Rho A inhibitor CT04, the Rac 1 inhibitor NSC23766, the PAK inhibitor FRAX597, or the Rock 2 inhibitor Y27632 to co-treat ADSCs, stress fiber formation is significantly reduced, resulting in decreased cell migration. Our findings may provide a new mechanism by which PRP promotes ADSC migration.

Acknowledgements

This work was supported by the Natural Science Foundation of China (81371719, 81472166, 81571860, and 81402613), the Colleges Pearl River Scholar Funded Scheme (GDUPS2013 and GDUPS2015), Guangzhou science and technology Foundation (201604020002), Guangdong Natural Science Foundation (2014A030312013) and Science and Technology Key Project of Guangdong Province (2014B020212010, 2015B020233012).

Disclosure of conflict of interest

None.

Address correspondence to: Biao Cheng, Department of Plastic Surgery, General Hospital of Southern Theater Command, PLA, Guangzhou 510010, China. Tel: +86-13889903217; E-mail: chengbiaocheng@163.com

References

[1] Nguyen DT, Orgill DP and Murphy GF. The pathophysiologic basis for wound healing and cutaneous regeneration. Biomaterials for Treating Skin Loss 2009; 25-57.

[2] Chong EJ, Phan TT, Lim IJ, Zhang YZ, Bay BH, Ramakrishna S and Lim CT. Evaluation of electrospun PCL/gelatin nanofibrous scaffold for wound healing and layered dermal reconstitution. Acta Biomater 2007; 3: 321-330.

[3] Nardi NB and da Silva Meirelles L. Mesenchymal stem cells: isolation, in vitro expansion and characterization. Stem cells. Springer; 2008. pp. 249-282.

[4] Ong WK and Sugii S. Adipose-derived stem cells: fatty potentials for therapy. Int J Biochem Cell Biol 2013; 45: 1083-1086.

[5] Kloskowski T, Kowalczyk T, Nowacki M and Drewa T. Tissue engineering and ureter regeneration: is it possible? Int J Artif Organs 2013; 36: 392-405.

[6] Naderi N, Combellack EJ, Griffin M, Sedaghati T, Javed M, Findlay MW, Wallace CG, Mosahebi A, Butler PE, Seifalian AM, Whitaker IS. The regenerative role of adipose-derived stem cells (ADSC) in plastic and reconstructive surgery. Int Wound J 2016; 14: 112-124.

[7] Zuk PA, Zhu M, Mizuno H, Huang J, Futrell JW, Katz AJ, Benhaim P, Lorenz HP and Hedrick MH. Multilineage cells from human adipose tissue: implications for cell-based therapies. Tissue Eng 2001; 7: 211-228.

[8] Hong SJ, Jia SX, Xie P, Xu W, Leung KP, Mustoe TA and Galiano RD. Topically delivered adipose derived stem cells show an activated-fibroblast phenotype and enhance granulation tissue formation in skin wounds. PLoS One 2013; 8: e55640.

[9] Liu S, Zhang H, Zhang X, Lu W, Huang X, Xie H, Zhou J, Wang W, Zhang Y and Liu Y. Synergistic

angiogenesis promoting effects of extracellular matrix scaffolds and adipose-derived stem cells during wound repair. Tissue Eng Part A 2010; 17: 725-739.
[10] Saucedo JM, Yaffe MA, Berschback JC, Hsu WK and Kalainov DM. Platelet-rich plasma. J Hand Surg 2012; 37: 587-589.
[11] Yu W, Wang J and Yin J. Platelet-rich plasma: a promising product for treatment of peripheral nerve regeneration after nerve injury. Int J Neurosci 2011; 121: 176-180.
[12] Borrione P, Di Gianfrancesco A, Pereira MT and Pigozzi F. Platelet-rich plasma in muscle healing. Am J Phys Med Rehabil 2010; 89: 854-861.
[13] Landesberg R, Roy M and Glickman RS. Quantification of growth factor levels using a simplified method of platelet-rich plasma gel preparation. J Oral Maxillofac Surg 2000; 58: 297-300.
[14] Foster TE, Puskas BL, Mandelbaum BR, Gerhardt MB and Rodeo SA. Platelet-rich plasma: from basic science to clinical applications. The Am J Sports Med 2009; 37: 2259-2272.
[15] Zhang L, Xu P, Wang X, Zhang M, Yan Y, Chen Y, Zhang L and Zhang L. Activin B regulates adipose-derived mesenchymal stem cells to promote skin wound healing via activation of the MAPK signaling pathway. Int J Biochem Cell Biol 2017; 87: 69-76.
[16] Raftopoulou M and Hall A. Cell migration: Rho GTPases lead the way. Dev Biol 2004; 265: 23-32.
[17] Irving JA and Lala PK. Functional role of cell surface integrins on human trophoblast cell migration: regulation by TGF-β, IGF-II, and IGFBP-1. Exp Cell Res 1995; 217: 419-427.
[18] Eriksson K, Magnusson P, Dixelius J, Claesson-Welsh L and Cross MJ. Angiostatin and endostatin inhibit endothelial cell migration in response to FGF and VEGF without interfering with specific intracellular signal transduction pathways. FEBS Lett 2003; 536: 19-24.
[19] Jiang Q, Zhou C, Bi Z and Wan Y. EGF-induced cell migration is mediated by ERK and PI3K/AKT pathways in cultured human lens epithelial cells. J Ocul Pharmacol Ther 2006; 22: 93-102.
[20] Okano I, Hiraoka J, Otera H, Nunoue K, Ohashi K, Iwashita S, Hirai M and Mizuno K. Identification and characterization of a novel family of serine/threonine kinases containing two N-terminal LIM motifs. J Biol Chem 1995; 270: 31321-31330.
[21] Hall A. Rho GTPases and the actin cytoskeleton. Science 1998; 279: 509-514.
[22] Yang N, Higuchi O, Ohashi K and Nagata K. Cofilin phosphorylation by LIM-kinase 1 and its role in Rac-mediated actin reorganization. Nature 1998; 393: 809.
[23] Sumi T, Matsumoto K, Takai Y and Nakamura T. Cofilin phosphorylation and actin cytoskeletal dynamics regulated by rho-and Cdc42-activated LIM-kinase 2. J Cell Biol 1999; 147: 1519-1532.
[24] Edwards DC, Sanders LC, Bokoch GM and Gill GN. Activation of LIM-kinase by Pak1 couples Rac/Cdc42 GTPase signalling to actin cytoskeletal dynamics. Nat Cell Biol 1999; 1: 253.
[25] Ohashi K, Nagata K, Maekawa M, Ishizaki T, Narumiya S and Mizuno K. Rho-associated kinase ROCK activates LIM-kinase 1 by phosphorylation at threonine 508 within the activation loop. J Biol Chem 2000; 275: 3577-3582.
[26] Dan C, Kelly A, Bernard O and Minden A. Cytoskeletal changes regulated by the PAK4 serine/threonine kinase are mediated by LIM kinase 1 and cofilin. J Biol Chem 2001; 276: 32115-32121.